2,000-year-old shipwreck reveals complex trade network

This file contains 3 documents:

1. Findings from 2,000-year-old Uluburun shipwreck reveal complex trade network

Using advanced geochemical analyses, a team of scientists has uncovered new answers to decades-old questions about trade of tin throughout Eurasia during the Late Bronze Age.

November 30, 2022

Source: https://www.sciencedaily.com/releases/2022/11/221130151458.htm

2. Tin from Uluburun shipwreck shows small-scale commodity exchange fueled continental tin supply across Late Bronze Age Eurasia

30 Nov 2022

Wayne Powell, Michael Frachetti, H. Arthur Bankoff, Gojko Barjamovic, Michael Johnson , Ryan Mathur, Vincent C. Pigott, Michael Price and K. Aslihan Yener, 2022. Science Advances, Vol 8, Issue 48, DOI: 10.1126/sciadv.abq3766

Source: https://www.science.org/doi/10.1126/sciadv.abq3766

3. Supplementary material

Source: https://www.science.org/doi/suppl/10.1126/sciadv.abq3766/suppl_file/sciadv.abq3766_sm.pdf

Assembled by Wergosum on 20221202

Findings from 2,000-year-old Uluburun shipwreck reveal complex trade network

More than 2,000 years before the Titanic sunk in the North Atlantic Ocean, another famous ship wrecked in the Mediterranean Sea off the eastern shores of Uluburun -- in present-day Turkey -- carrying tons of rare metal. Since its discovery in 1982, scientists have been studying the contents of the Uluburun shipwreck to gain a better understanding of the people and political organizations that dominated the time period known as the Late

Now, a team of scientists, including Michael Frachetti, professor of archaeology in Arts & Sciences at Washington University in St. Louis, have uncovered a surprising finding: small communities of highland pastoralists living in present-day Uzbekistan in Central Asia produced and supplied roughly one-third of the tin found aboard the ship -- tin that was en route to markets around the Mediterranean to be made into coveted bronze metal.

The research, published on November 30 in *Science Advances*, was made possible by advances in geochemical analyses that enabled researchers to determine with high-level certainty that some of the tin originated from a prehistoric mine in Uzbekistan, more than 2,000 miles from Haifa, where the ill-fated ship loaded its cargo.

But how could that be? During this period, the mining regions of Central Asia were occupied by small communities of highlander pastoralists -- far from a major industrial center or empire. And the terrain between the two locations -- which passes through Iran and Mesopotamia -- was rugged, which would have made it extremely difficult to pass tons of heavy metal.

Frachetti and other archaeologists and historians were enlisted to help put the puzzle pieces together. Their findings unveiled a shockingly complex supply chain that involved multiple steps to get the tin from the small mining community to the Mediterranean marketplace.

"It appears these local miners had access to vast international networks and -- through overland trade and other forms of connectivity -- were able to pass this all-important commodity all the way to the Mediterranean," Frachetti said.

"It's quite amazing to learn that a culturally diverse, multiregional and multivector system of trade underpinned Eurasian tin exchange during the Late Bronze Age."

Adding to the mystique is the fact that the mining industry appears to have been run by small-scale local communities or free laborers who negotiated this marketplace outside of the control of kings, emperors or other political organizations, Frachetti said.

"To put it into perspective, this would be the trade equivalent of the entire United States sourcing its energy needs from small backyard oil rigs in central Kansas," he said.

About the research

The idea of using tin isotopes to determine where metal in archaeological artifacts originates dates to the mid-1990s, according to Wayne Powell, professor of earth and environmental sciences at Brooklyn College and a lead author on the study. However, the technologies and methods for analysis were not precise enough to provide clear answers. Only in the last few years have scientists begun using tin isotopes to directly correlate mining sites to assemblages of metal artifacts, he said.

"Over the past couple of decades, scientists have collected information about the isotopic composition of tin ore deposits around the world, their ranges and overlaps, and the natural mechanisms by which isotopic compositions were imparted to cassiterite when it formed," Powell said. "We remain in the early stages of such study. I expect that in future years, this ore deposit database will become quite robust, like that of Pb isotopes today, and the method will be used routinely."

Aslihan K. Yener, a research affiliate at the Institute for the Study of the Ancient World at New York University and a professor emerita of archaeology at the University of Chicago, was one of the early researchers who conducted lead isotope analyses. In the 1990s, Yener was part of a research team that conducted the first lead isotope analysis of the Uluburun tin. That analysis suggested that the Uluburun tin may have come from two sources -- the Kestel Mine in Turkey's Taurus Mountains and some unspecified location in central Asia.

"But this was shrugged off since the analysis was measuring trace lead and not targeting the origin of the tin," said Yener, who is a co-author of the present study.

Yener also was the first to discover tin in Turkey in the 1980s. At the time, she said the entire scholarly community was surprised that it existed there, right under their noses, where the earliest tin bronzes occurred.

Some 30 years later, researchers finally have a more definitive answer thanks to the advanced tin isotope analysis techniques: One-third of the tin aboard the Uluburun shipwreck was sourced from the Mušiston mine in Uzbekistan. The remaining two-thirds of the tin derived from the Kestel mine in ancient Anatolia, which is in present-day Turkey.

Findings offer glimpse into life 2,000-plus years ago

By 1500 B.C., bronze was the "high technology" of Eurasia, used for everything from weaponry to luxury items, tools and utensils. Bronze is primarily made from copper and tin. While copper is fairly common and can be found throughout Eurasia, tin is much rarer and only found in specific kinds of geological deposits, Frachetti said.

"Finding tin was a big problem for prehistoric states. And thus, the big question was how these major Bronze Age empires were fueling their vast demand for bronze given the lengths and pains to acquire tin as such a rare commodity. Researchers have tried to explain this for decades," Frachetti said.

The Uluburun ship yielded the world's largest Bronze Age collection of raw metals ever found -- enough copper and tin to produce 11 metric tons of bronze of the highest quality. Had it not been lost to sea, that metal would have been enough to outfit a force of almost 5,000 Bronze Age soldiers with swords, "not to mention a lot of wine jugs," Frachetti said.

"The current findings illustrate a sophisticated international trade operation that included regional operatives and socially diverse participants who produced and traded essential hard-earth commodities throughout the late Bronze Age political economy from Central Asia to the Mediterranean," Frachetti said.

Unlike the mines in Uzbekistan, which were set within a network of small-scale villages and mobile pastoralists, the mines in ancient Anatolia during the Late Bronze Age were under the control of the Hittites, an imperial global power of great threat to Ramses the Great of Egypt, Yener explained.

The findings also show that life 2,000-plus years ago was not that different from what it is today.

"With the disruptions due to COVID-19 and the war in Ukraine, we have become aware of how we are reliant on complex supply chains to maintain our economy, military and standard of living," Powell said. "This is true in prehistory as well. Kingdoms rose and fell, climatic conditions shifted and new peoples migrated across Eurasia, potentially disrupting or redistributing access to tin, which was essential for both weapons and agricultural tools.

"Using tin isotopes, we can look across each of these archaeologically evident disruptions in society and see connections were severed, maintained or redefined. We already have DNA analysis to show relational connections. Pottery, funerary practices, etc., illustrate the transmission and connectivity of ideas. Now with tin isotopes, we can document the connectivity of long-distance trade networks and their sustainability."

More clues to explore

The current research findings settle decades-old debates about the origins of the metal on the Uluburun shipwreck and Eurasian tin exchange during the Late Bronze Age. But there are still more clues to explore.

After they were mined, the metals were processed for shipping and ultimately melted into standardized shapes -- known as ingots -- for transporting. The distinct shapes of the ingots served as calling cards for traders to know from where they originated, Frachetti said.

Many of the ingots aboard the Uluburun ship were in the "oxhide" shape, which was previously believed to have originated in Cyprus. However, the current findings suggest the oxhide shape could have originated farther east. Frachetti said he and other researchers plan to continue studying the unique shapes of the ingots and how they were used in trade.

In addition to Frachetti, Powell and Yener, the following researchers contributed to the present study: Cemal Pulakat at Texas A&M University, H. Arthur Bankoff at Brooklyn College, Gojko Barjamovic at Harvard University, Michael Johnson at Stell Environmental Enterprises, Ryan Mathur at Juniata College, Vincent C. Pigott at the University of Pennsylvania Museum and Michael Price at the Santa Fe Institute.

The study was funded in part by a Professional Staff Congress-City University of New York Research Award, in addition to a research grant from the Institute for Aegean Prehistory.

ANTHROPOLOGY

Tin from Uluburun shipwreck shows small-scale commodity exchange fueled continental tin supply across Late Bronze Age Eurasia

Wayne Powell[1,2]*, Michael Frachetti[3,4]*, Cemal Pulak[5], H. Arthur Bankoff[6], Gojko Barjamovic[7], Michael Johnson[8], Ryan Mathur[9], Vincent C. Pigott[10], Michael Price[11], K. Aslihan Yener[12]

This paper provides the first comprehensive sourcing analysis of the tin ingots carried by the well-known Late Bronze Age shipwreck found off the Turkish coast at Uluburun (ca. 1320 BCE). Using lead isotope, trace element, and tin isotope analyses, this study demonstrates that ores from Central Asia (Uzbekistan and Tajikistan) were used to produce one-third of the Uluburun tin ingots. The remaining two-thirds were derived from the Taurus Mountains of Turkey, namely, from stream tin and residual low-grade mineralization remaining after extensive exploitation in the Early Bronze Age. The results of our metallurgical analysis, along with archaeological and textual data, illustrate that a culturally diverse, multiregional, and multivector system underpinned Eurasian tin exchange during the Late Bronze Age. The demonstrable scale of this connectivity reveals a vast and disparate network that relied as much on the participation of small regional communities as on supposedly hegemonic institutions of large, centralized states.

INTRODUCTION

By 1500 BCE, bronze was the "high technology" of Eurasia. Iconic ancient states, such as the Shang (China), Mycenean (Greece), and Assyrian (Iraq), used bronze for military power and social prestige, as well as for common tools and utensils. During this period, small- and large-scale communities sought access to its main components: copper and tin. Copper was relatively abundant throughout Eurasia, with porphyry copper ores occurring throughout the Pontic-Caucasus-Zagros mountains, sedimentary copper deposits in eastern Egypt and the Levant, and volcanogenic deposits in Cyprus. Given this wide distribution, copper deposits lay within reach for all major states of the Eastern Mediterranean and Near East. Tin, however, is more than 30 times less abundant than copper in the Earth's crust (*1*), and conditions under which tin deposits form are geologically limited. Furthermore, unlike copper, most deposits of tin lay far from major urban centers of the ancient world. Throughout the second millennium BCE, the acquisition of tin was thus a strategic military and economic endeavor, comparable to crude oil today. As a result, scholars have long speculated about the ore sources and exchange trajectories that funneled tin across Eurasia toward major markets of consumption during the Late Bronze Age (LBA; ca. 1650 to 1200 BCE) (*2*).

[1]Department of Earth and Environmental Sciences, Brooklyn College, Brooklyn, NY 11210, USA. [2]Earth and Environmental Sciences Program, The Graduate Center, New York, NY 10016, USA. [3]Department of Anthropology, Washington University in St. Louis, St. Louis, MO 63130, USA. [4]School of Cultural Heritage, Northwest University, No. 229 Taibai Road, Xi'an, Shaanxi Province, China. [5]Institute of Nautical Archaeology at Texas A&M University, College Station, TX 77843, USA. [6]Department of Anthropology, Brooklyn College, Brooklyn, NY 11210, USA. [7]Department of Near Eastern Languages and Civilizations, Harvard University, Cambridge, MA 01238, USA. [8]Stell Environmental Enterprises, Exton, PA 19341, USA. [9]Geology Department, Juniata College, Huntingdon, PA 16652, USA. [10]Asian Section, University of Pennsylvania Museum, Philadelphia, PA 19104, USA. [11]Michael Price, Santa Fe Institute, Santa Fe, MN 87506, USA. [12]Institute for the Study of the Ancient World at New York University (ISAW), New York, NY 10028, USA.
*Corresponding author. Email: wpowell@brooklyn.cuny.edu (W.P.); frachetti@wustl.edu (M.F.)

Here, we document the confluence of distant tin ore sources among the cargo of the Uluburun shipwreck. Excavations of the LBA shipwreck [1320 cal. BCE ± 15 2σ (*3*)], found off the coast of Turkey (Fig. 1), yielded the world's largest Bronze Age assemblage of raw metals ever found (*4*). The ship's primary cargo consisted of 10 metric tons (MT) of Cypriot copper ingots (*5*) and a staggering 1 MT of tin ingots, easily the largest and most securely dated collection of ancient tin metal known worldwide (*6*). Archaeologists and historians have long sought to trace the sources of tin needed by rival Mediterranean empires, whose expansive imperial goals demanded powerful war machines by the LBA. These empires, embroiled in extensive political conflict and warfare, were important metal consumers with demand likely exceeding hundreds of metric tons per year. Using the common LBA ratio of 9 parts copper to 1 part tin, the Uluburun tin cargo could have produced 11 MT of bronze of the highest quality, enough to outfit a force of almost 5000 Bronze Age soldiers with swords.

While tin was arguably the most critical hard commodity in Eurasia for over 2000 years, the exact sources of tin and its distribution networks across Eurasia have remained largely speculative, with few exceptions. Here, we provide the first comprehensive analysis of 105 tin ingots from the Uluburun shipwreck (91% of the total tin cargo) using a combined methodology of Pb isotope, trace element, and Sn isotope analyses. This systematic approach permits reexamination of the possible sources of Uluburun tin and demonstrates that the composition of two-thirds of the ingots is consistent with a source in the nearby Taurus Mountains of Turkey. In addition, we document the chemical fingerprints of the remaining one-third ($n = 35$) of the tin ingots, tracing them to ore deposits in Tajikistan and Uzbekistan, over 3000 km east of their final resting place.

The geochemical analysis of the Uluburun tin ingots reveals that the ores were not only sourced from vastly distant locations but that these regional ores converged to supply the bronze trade in the Mediterranean. Coupled with tin's geological rarity, geographic distance from major ancient population centers, and logistical complexity to procure, the tin ingots from Uluburun thereby index a

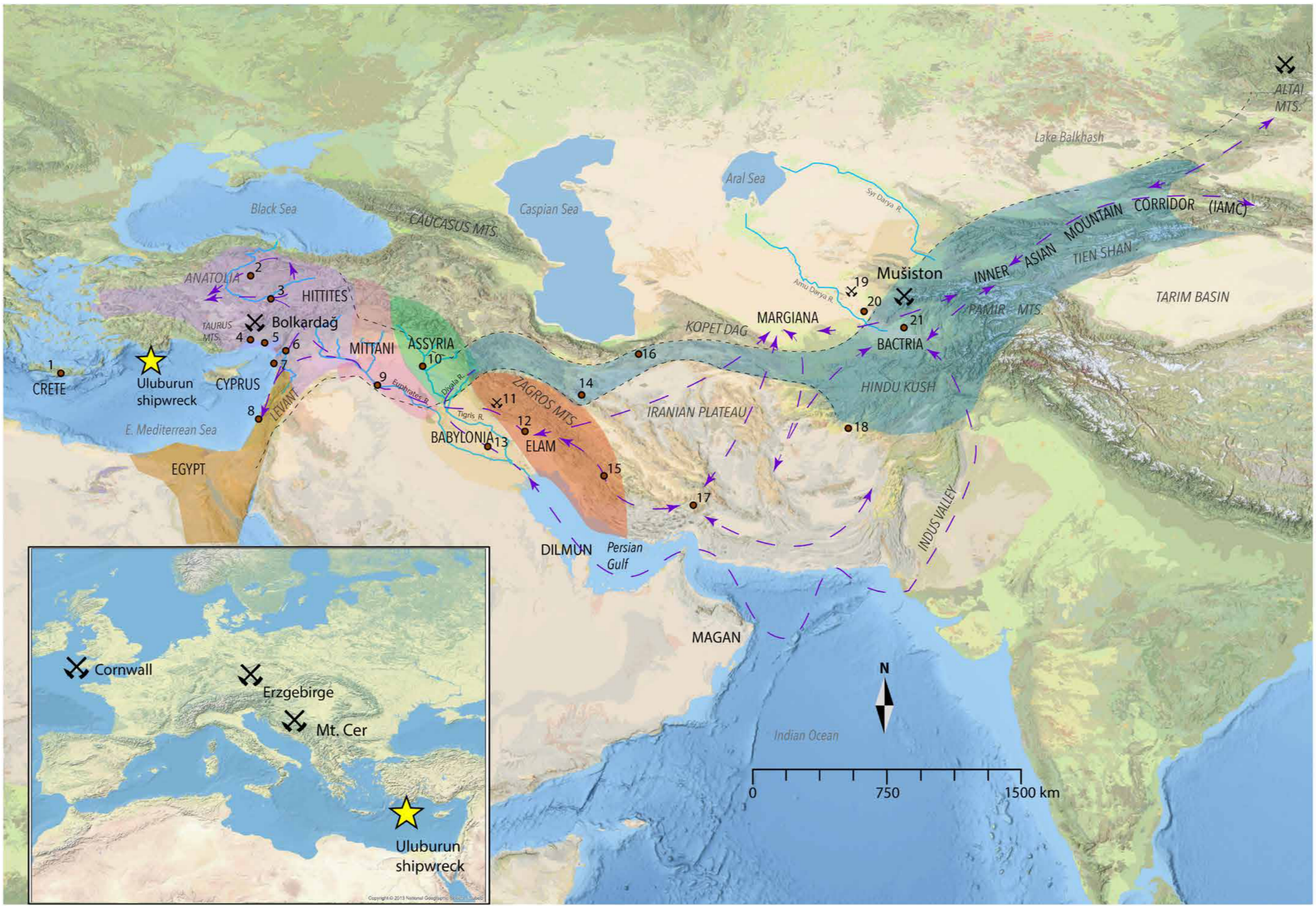

Fig. 1. Regional geography and main sites. 1, Hagia Triada; 2, Hattusa; 3, Hisarcık; 4, Mersin; 5, Tarsus; 6, Alalakh; 7, Ugarit; 8, Haifa; 9, Mari; 10, Assur; 11, Deh Hosein; 12, Susa; 13, Ur; 14, Arisman; 15, Tal-e Malyan; 16, Tepe Hissar; 17, Tepe Yahya; 18, Mundigak; 19, Karnab/Sichkonchi; 20, Sapalli; 21, Shortugai. Purple dashed arrows depict documented trade networks ca. 2200 to 1700 BCE. Blue shaded region reflects the corridor connecting the Anatolian and Central Asian/Middle Eastern tin trade (in blue), ca. 1600 to 1000 BCE. Other shaded areas represent key LBA polities. Inset map illustrates the location of ancient tin sources in Europe.

vast interconnected landscape of regional operatives and socially diverse participants who produced and traded essential hard-earth commodities throughout the LBA political economy from Central Asia to the Mediterranean in the late second millennium BCE. Ultimately, our findings suggest that LBA tin exchange required participation of communities ranging from small-scale highland populations to urbanized states to meet the abundant demand for bronze, which stimulated long-distance connectivity between Near Eastern urban centers and mining communities from Anatolia to Central Asia.

RESULTS

All 105 Uluburun tin ingots analyzed yield $^{208}Pb/^{204}Pb$ values that are consistent with Late Paleozoic to Cenozoic ores, except for KW 0516, which was derived from an older source. Tin isotope ($\delta^{124}Sn$) values span ~2 per mil (‰) from −0.88 to 1.24‰ with a median of 0.70‰ (table S1). Organizing the data according to their isotopic signature and their geological age allows for the identification of eight ingot groupings (Fig. 2B): three derived from Late Paleozoic ores (P1, P2A, and P2B) and five from a Late Mesozoic to Cenozoic source (MC1A, MC1B, MC1C, MC2A, and MC2B). Blind clustering of samples using *t*-distributed stochastic neighbor embedding (*t*-SNE) analysis statistically verified these groups (Fig. 3), where the four variables input to the *t*-SNE algorithm reflect independent aspects of the metal: $^{208}Pb/^{204}Pb$, $\delta^{124}Sn$, $^{206}Pb/^{204}Pb$ Pb inputs, and Pb concentration.

DISCUSSION

Mesozoic-Cenozoic ore groups

The Uluburun tin cargo includes a morphologically diverse (oxhide, slab, bun, and stone anchor shaped; Fig. 4) group of Pb-enriched ingots (MC1) that were produced from ores collected in the Taurus region and subsequently pooled and smelted at the nearby Pb-Ag mining center of Bolkardağ where extraneous Pb was added (*7*). Comparison of median $\delta^{124}Sn$ from tin ingots and tin ores from across Europe and Central Asia (*8*) further supports this conclusion, with 49 Pb-enriched ingots being comparable to the Taurus tin ores of Kestel and Hisarcık (Fig. 5). This is also true for 11 oxhide and slab ingots (MC2) with $^{208}Pb/^{204}Pb$ consistent with slightly older mineralization in the Taurus Mountains, likely Aladağ. Note that

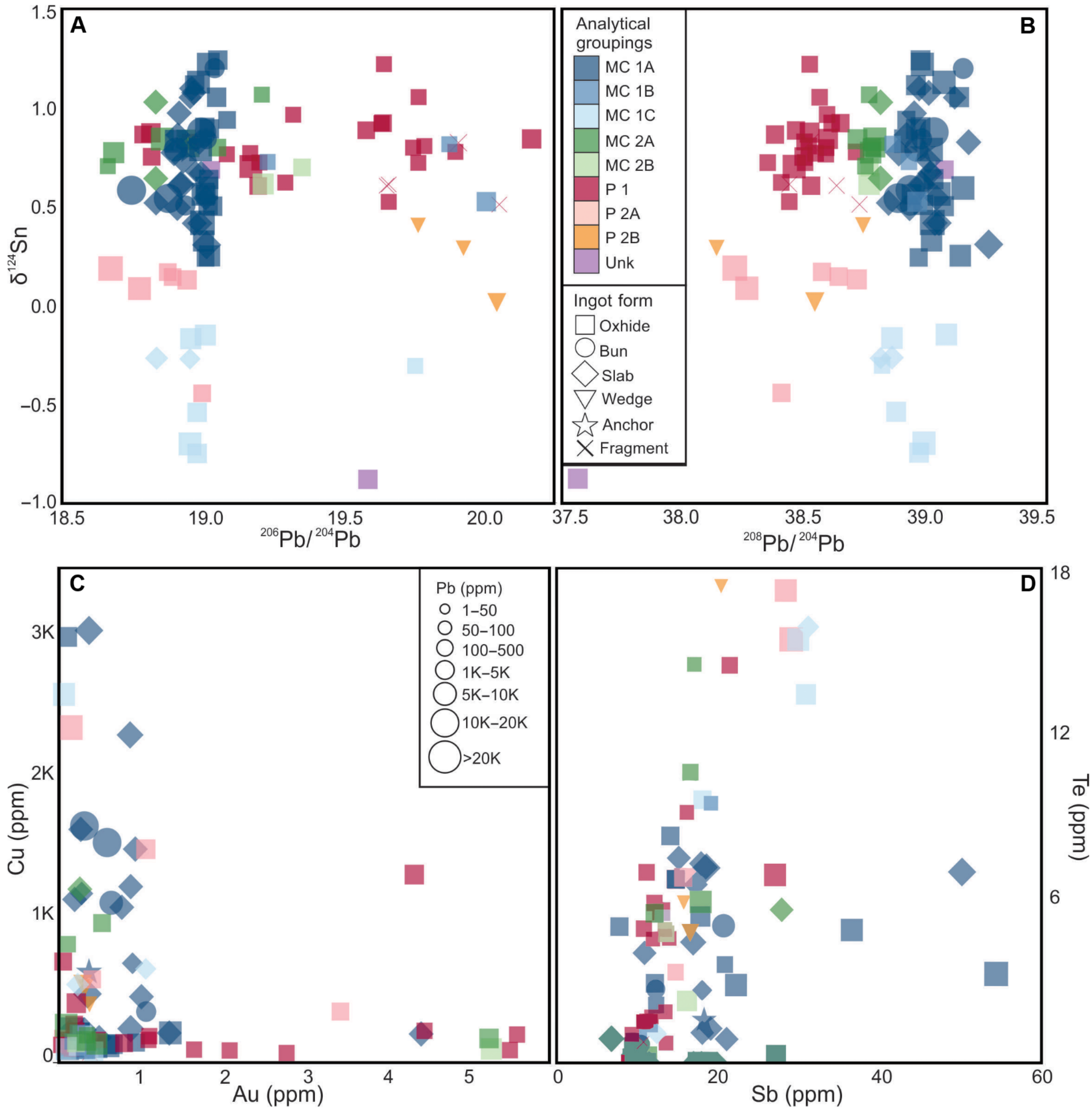

Fig. 2. Cross-plots of Uluburun tin ingot compositions. (**A**) δ^{124}Sn versus ^{206}Pb/^{204}Pb; (**B**) δ^{124}Sn versus ^{208}Pb/^{204}Pb; (**C**) Cu versus Au; (**D**) Sb versus Te. Analytical groupings correspond to isotopic and chemical composition correlated with age: MC, Mesozoic-Cenozoic; P, Paleozoic; Unk, unknown; icon shape corresponds to ingot form; icon size reflects Pb concentration. Note that axes in (D) are limited to 60 parts per million (ppm) of Sb for readability, thereby omitting three bun ingots with Sb > 100 ppm (KW 199, KW 847, and KW 1326). Similarly, samples KW 198, KW 199, and KW 2874 with Cu > 5800 ppm were omitted.

while Serbian tin ores are similar in composition to the MC2 group, the extent of exchange of tin from this small deposit is archaeologically conscribed within west-central Serbia (*9*).

Group MC1C is defined as a subset of seven Bolkardağ-derived ingots (oxhide and slab) with negative δ^{124}Sn values (Fig. 5). The polymetallic ores of Bolkardağ include stannite (Cu_2FeSnS_4) (*10*), a mineral typically associated with negative Sn isotopic values (*11*), and the analysis of one sample of stannite form Bolkardağ ore yielded a δ^{124}Sn value of −1.94‰, although further work is required to document the true range of values associated with these ores. Hydrostannates such as mushistonite {[Cu, Zn, Fe]Sn$(OH)_6$} and cassiterite (SnO_2) are the ultimate weathering products of stannite (*12*, *13*) and may have accumulated in nearby river sediments (*14*). Furthermore, given the greater bond strength of Sn in the oxidized product, the Sn isotopic composition of the oxides would shift somewhat to higher values. Accordingly, the most likely known source for group MC1C is the Maden stream, which flows below the polymetallic mineralization of Bolkardağ. Thus, 68 Uluburun tin ingots (65%) are interpreted to have been produced in the Taurus Mountains of Turkey.

Paleozoic ores groups

Lead isotope analysis (LIA) indicates that 35 of the remaining ingots were derived from Late Paleozoic ores. Twenty-six of these samples (group P1) are characterized by moderate to high δ^{124}Sn (median, 0.79‰) and variable enrichment in ^{206}Pb and were cast in the oxhide

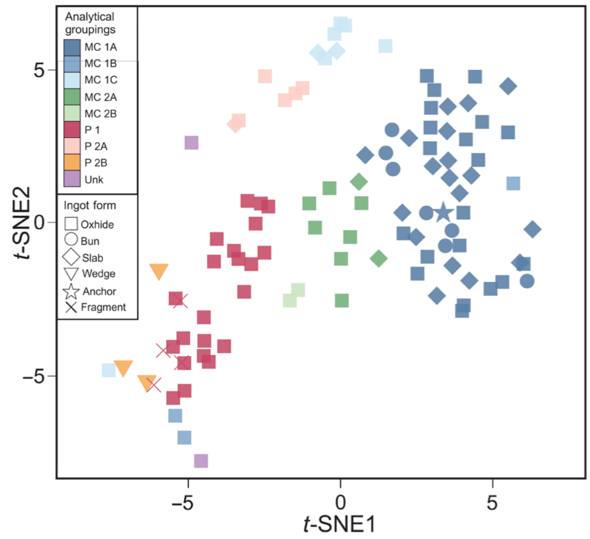

Fig. 3. Two-dimensional *t*-SNE plot showing visual clusters of proximal points (samples). The input variables to the *t*-SNE algorithm were three isotopic ratio measurements for lead and one for tin (position), corresponding to defined analytical groupings (color) and ingot form (shape). Analytical groupings correspond to isotopic and chemical composition correlated with age: MC, Mesozoic-Cenozoic; P, Paleozoic; Unk, unknown; icon shape corresponds to ingot form.

form. High Au, low Cu, Ag, and Pb and incorporation of radiogenic ^{206}Pb suggest a placer origin.

Nine samples (group P2) have low δ^{124}Sn (median, 0.14‰): Three wedge-shaped ingots (P2B) are enriched in ^{206}Pb but not the six oxhide ingots (P2A). As with P1, the chemical signature suggests that P2B was derived from stream tin. The only documented Late Paleozoic tin sources with comparably low δ^{124}Sn are the stannite and secondary cassiterite-bearing Mušiston deposit in Tajikistan and deposits in the eastern Altai region of Kazakhstan (Fig. 5).

The provenance of the two remaining tin ingots is uncertain. The ^{208}Pb/^{204}Pb value of KW 0516 indicates a non-European Late Precambrian source. Sample KW 0403 exhibits unusually high ^{207}Pb/^{204}Pb decoupled from ^{206}Pb/^{204}Pb and does not align with currently documented Eurasia sites.

Tin and lead compositional ranges for P1 ingots overlap with tin ores from Cornwall, Sardinia, Erzgebirge, and the Tien Shan Mountains. However, additional constraints narrow the list of potential candidates. Erzgebirge tin trade did not extend to the Mediterranean or Black Sea (*8*, *14*), making it an unlikely contributor to the Uluburun shipwreck tin ingot assemblage. Many of the Uluburun tin ingots, including stannite-associated samples (Mušiston and Bolkardağ) and a subset of P1 ingots, exhibit elevated concentrations of Te compared to the average crustal abundance of 0.03 parts per million (ppm) (*15*). Tellurium enrichment is associated with epithermal mineralization systems (<1-km depth) (*16*), consistent with the 0.5- to 3-km depth of Central Tajikistan's polymetallic tin deposits (*17*). The lode and greisen ores of Cornwall formed at greater depths (2.5 to 6 km) (*18*); the single Te analysis from the English tin ingots has <1.3 ppm of Te; and the P1 group lacks the correlation between Pb, Bi, Sb, and In observed in the Salcombe tin ingot assemblage (*19*). Thus, Central Asia is a more likely origin than Britain for the ingots in question.

The predominantly oxhide form of the P1 tin ingots may provide an additional clue to their provenance. Copper ingots of this form have been documented over a vast area from southern France and Central Germany to central Iraq but are absent from the British Isles (*20*). By the 14th century BCE, copper oxhide ingots had become a Cypriot "commodity brand" (*20*), but the origin of the form predates its adoption in Cyprus. The oldest securely dated full-size copper oxhide ingots have been found on Crete and date to ca. 1500 to 1450 BCE (*20*). LIA indicates that some of these were derived from non-European copper, possibly from Anatolia, Afghanistan, Iran, Southern Russian, or Central Asia (*21*). This raises the possibility that the oxhide form was not indigenous to the Mediterranean but originated farther east (*21*). The presence of Te-enriched examples and oxhide form of the P1 Uluburun tin ingots, along with the presence of Mušiston-derived tin (P2) within the Uluburun cargo, points to a Central Asian origin for the 26 P1 ingots.

LBA tin and the tin trade

What is known about the tin trade in the ancient Near East is based mainly on commercial records from the 19th century BCE found at the central Anatolian site of Kültepe. Written on clay tablets in the cuneiform script five centuries before the Uluburun ship, these texts document an extensive trade in tin ingots and textiles between Mesopotamia and Anatolia but provide only ambiguous references to tin arriving in Mesopotamian from the east (*1*). There are a handful of Assyrian records contemporaneous with the Uluburun ship that refer to trade in tin from Anatolia to Iraq (*22*), but no textual evidence definitively identifies localities from which tin was mined.

Numerous tin deposits have been identified in areas east of the great Bronze Age population centers in Iraq. Those in Afghanistan lack evidence of ancient exploitation (*23*), but copper ore containing cassiterite was mined at Deh Hosein in Iran during the second millennium BCE (*24*). In addition, numerous tin mines and smelting sites dating to the 18th to 11th centuries BCE have been excavated in Kazakhstan (*25*) and, from ca. 2600 to 1250 BCE, in Uzbekistan and Tajikistan (*26*) including the unique stannite-rich mine at Mušiston. Looking westward, tin production sites dating from ca. 3000 to 2000 BCE have been found at Kestel and Hisarcık in south-central Anatolia (Fig. 6) (*9*, *27*, *28*), and placer ores were worked across LBA Europe, including Bohemia-Saxony (*29*), Serbia (*30*), and Cornwall (*19*). With the exception of Anatolia, where tin ores lay within the provincial territory of Hatti, the identified tin ores lie within regions with no identified Bronze Age state formation.

Both ancient texts and archaeology of Central and Western Asia provide insight concerning the apparatuses that supported a vast, interregional network of metallurgical production and transport across this region. Excavations in the mining site of Mušiston (Tajikistan) show that the populations that worked the tin mines were probably seasonal inhabitants supported by a combination of seasonal herding and connectivity with lowland agricultural communities (*26*, *31*). Cities in the adjacent lowlands reached their apogee in the Middle Bronze Age (ca. 2000 to 1500 BCE) and subsequently entered a period of decline in the LBA (*32*). However, during the LBA, this region saw the fluorescence of less aggregated, small-scale settlements, suggesting a shift toward more diversified economic strategies ranging from mobile pastoralism to more integrated forms of agricultural production (*33*). Ecologically situated pastoralist systems coupled with context-specific farming hamlets shaped a complex network of interacting communities concentrated in the piedmont regions of the Inner Asian Mountain Corridor (IAMC). This interaction entangled local communities from the northern edges of the

Fig. 4. Representative forms of tin ingots from the cargo of the Uluburun shipwreck.

Iranian Plateau through the Pamir and Tien Shan foothills eastward toward China and northward to the Altai mountains in shared networks of resource exchange (*34*–*36*).

After ca. 1500 BCE, the archaeological data suggest a period of considerable and renewed connectivity in terms of commodities and technologies throughout the IAMC (*37*). The northeastward transmission of a range of regionally sourced materials, including ceramics (*38*), textiles (*39*), and newly introduced domesticated crops (*40*), all demonstrate that large networks of contact existed among communities living north-south throughout the piedmont regions of Inner Asia in the late second millennium BCE (*41*). Human genomic data identify increased regional admixtures among Central Eurasian populations throughout the second millennium BCE, establishing clines of admixed central steppe ancestry that spanned throughout the IAMC as far south as the Indus region by 1000 BCE (*42*, *43*).

Research concerning the metallurgical networks that fueled tin-bronze production throughout the IAMC fits documented transmissions in other materials and ideas. The archaeological remains recovered from Mušiston and nearby tin mines at Karnab (Uzbekistan) consist of small-scale occupations and incised coarse-ware ceramics that are typologically similar to those documented among

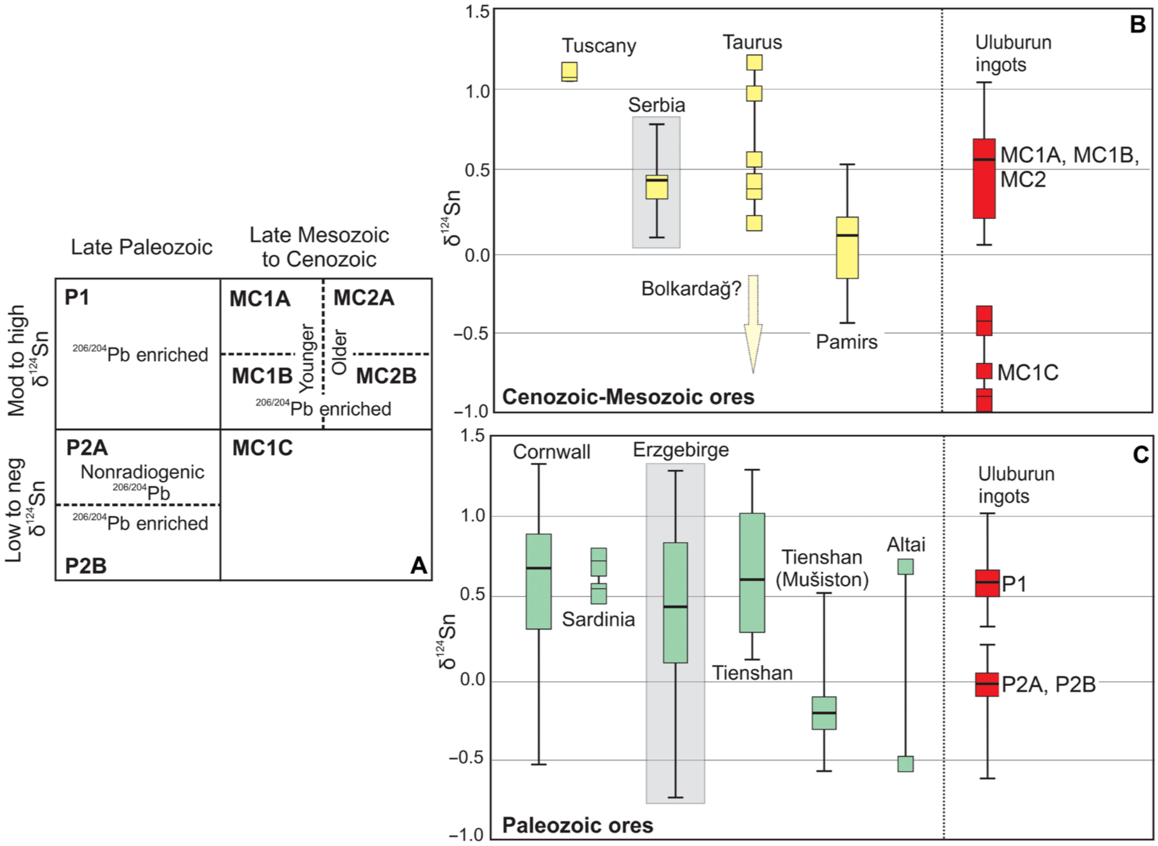

Fig. 5. Characteristics of ingots used to define groupings and comparison of δ^{124}Sn ranges of tin ores from Europe, Anatolia, and Central Asia. (**A**) Isotopic characteristics of ingot groupings; (**B**) Mesozoic-Cenozoic ores and corresponding ingots; (**C**) Paleozoic ores and corresponding ingots. Boxes illustrate the range of the second and third quartiles, and the median is marked with a horizontal line. δ^{124}Sn values of the ingots have been adjusted by −0.2‰ to compensate for fractionation during evaporative tin loss during the smelting process (*8*, *9*). Ores shown to have no presence in the LBA Mediterranean (*9*) are grayed out. Ore data compiled from the work of Berger *et al.* (*51*), Mason *et al.* (*9*), and this study. Note that the δ^{124}Sn values for ores have been reduced to account for the by +0.2‰ fractionation associated with smelting (*7*, *8*).

contemporary agropastoralists of the steppes/IAMC. Evidence for mining technology in the form of stone hammers and small-scale smelting operations is known from settlements along the IAMC from at least 1800 BCE (*44*). Analysis of bronze metals suggests that, by the LBA, bronze production relied on sourcing from a wide range of ores throughout the mountains of the IAMC (*25*). Similarly structured, small-scale communities may also have been engaged in tin trade from Muširton (and nearby sources) southward and westward across the Iranian Plateau (*45*). However, the connectivity between the mountainous regions of Inner Asia and Southwest Asia (Iran, Iraq, and the Levant) is less well documented in the LBA. Of notable importance, however, is the rise of communities sometimes described as "mountain tribes," living in the northern highlands of the Iranian Plateau, as well as along the westward piedmont of the Hindu Kush.

Textual evidence from the 19th century BCE for a commercial network moving tin from Central Asia to Mesopotamia is likewise robust (*1*), but the documentation dries up by the 16th century BCE, and chemical analyses of archaeological material from southern Iraq a few centuries later suggest that after 1500 BCE, the region relied mainly on the reuse and recycling of bronze (*46*). Therefore, the origin of the tin ingots from the Uluburun shipwreck demonstrates the continuation of large-scale commercial connections between Central Asia and the Mediterranean in the LBA, perhaps by way of transport routes that circumvented southern Mesopotamia for political reasons.

The potential vectors and transport routes from ancient Bactria (Fig. 1) across the Iranian Plateau have been considered by scholars for decades. The piedmont steppes of northern Iran provide a near-continuous and logical geography linking the mountain pastoralists of the Hindu Kush, Pamir, and Tien Shan to the Bactria-Margiana Archaeological Complex and westward across Iran [e.g., (*41*)]. Laursen and Steinkeller (*47*) describe the trade networks across Iran and the Persian Gulf in the Early and Middle Bronze Ages, suggesting that what has been termed the "Great Khorasan Road" was likely already in operation for the tin trade. The Uluburun cargo demonstrates that the land route continued through the LBA, connecting it to the documented evidence from the Middle Bronze Age (*1*) and suggesting that the Indian Ocean routes may have diminished.

Tin from Turkey

Fundamentally different scales of organization existed between central Asian and Taurus tin production. The recognition of tin ingots from the Uluburun shipwreck with Bolkardağ signatures suggests the existence of a significantly larger and longer-lived tin industry in the south-central Taurus than previously assumed. The available data point to a model of decentralized mining at disparate locations

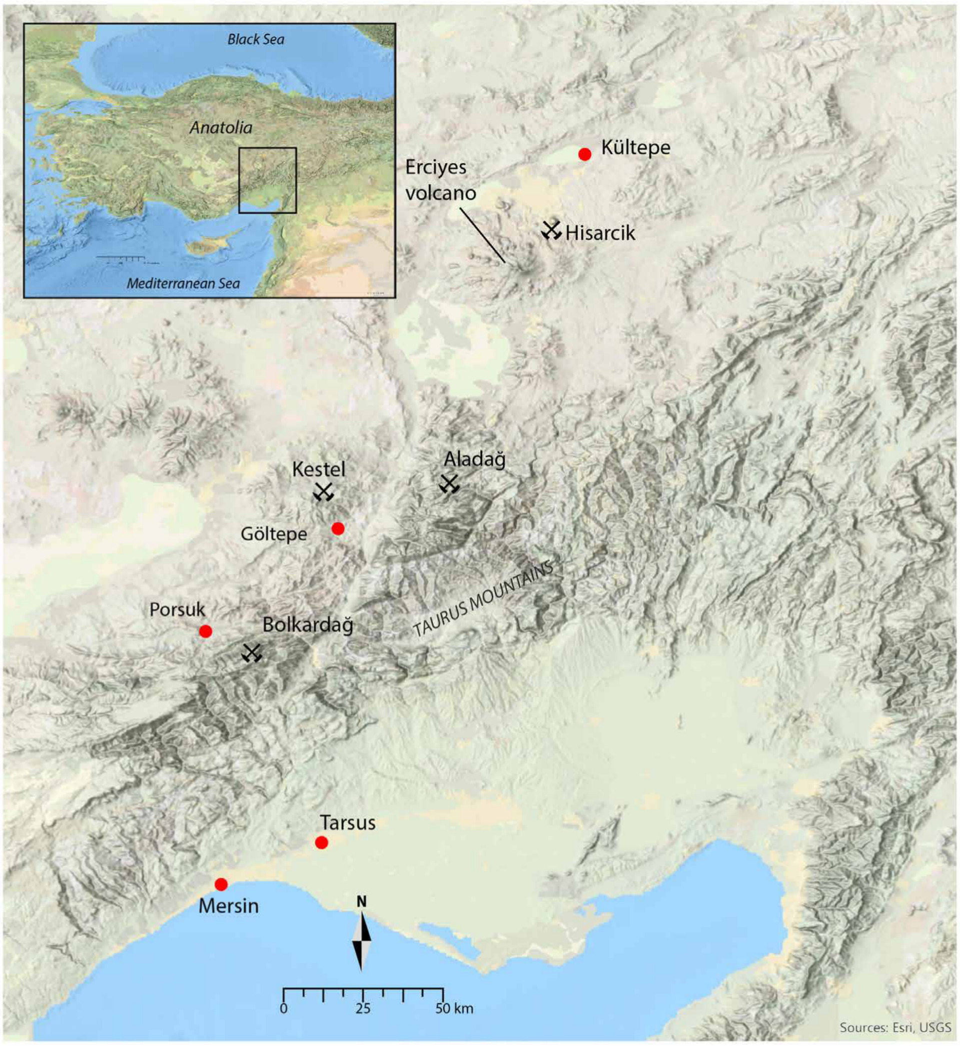

Fig. 6. Regional geography and main sites of south-central Anatolia.

that took advantage of atypical and smaller dispersed tin deposits. Tin ore or raw metal from multiple sources was agglomerated at strategically located hubs close to the tin sources such as the LBA Bolkardağ site of Porsuk at the head of the main Taurus passes (Fig. 6). From primary and secondary transshipment centers, ingots could be brought down to Mediterranean seaports located roughly 1 week away and loaded onto merchantmen such as the Uluburun ship.

Physical evidence of tin circulation within Anatolia is less visible. Sporadic evidence of an intra-Anatolian exchange comes from tax records found at the Hittite state capital (*48*) that are contemporary with the Uluburun shipwreck. These texts point to the accumulation of tin at the provincial capital of Kizzuwatna near the mining areas before the metal was shipped to the imperial capital of Hattusha, 2 weeks distant. International overland trade in Anatolian tin to Assyria and Babylonia (*22*) is documented in texts found at Assur in modern-day Iraq. Presumably, it converged with tin coming from the eastern network that also contributed tin to the Uluburun cargo. A greater degree of Hittite state oversight of Anatolian tin is suggested by these texts, differing from the dispersed nomadic model proposed for Mušiston.

Our analysis of the Uluburun tin ingots reliably documents multiple geographic sources of tin supplying the Mediterranean market for LBA bronze production. Roughly 30% of the Uluburun tin is sourced geologically to Central Asia, demanding a reassessment of the social and economic complexity reflected across diverse modes of political and social organization from the mines to the markets, and ultimately traded on seafaring vessels. The unexpectedly large percentage of tin from the Taurus Mountains (>65%) also requires a reconsideration of the importance of small-scale producers exploiting residual mineralization from previously exploited ores and placer deposits to fuel the major metallurgical industries that underpinned LBA Mediterranean societies and beyond.

While eastern sources of tin have been long speculated in archaeological debates, our data reveal a more socially diverse, multiregional, and multivector system underlying Eurasian tin trade. Anatolia, on whose southern shore the Uluburun ship had foundered, has rarely been suggested as a tin source. However, for Central Asia, a long-proposed source region, the exact provenience for traded tin had never before been documented. Our analysis exposes the complex geography, regional range, and social integrations that characterized

LBA tin trade, a necessary element for the effective production of bronze, a fundamental technology for millennia across Eurasia and beyond.

MATERIALS AND METHODS

A total of 105 Uluburun tin ingots (98% of the preserved metallic tin ingots) were analyzed. Metal shavings were extracted from the nonweathered cores of ingots using a 6-mm high-speed steel (HSS) twist drill bit. All granular and nonmetallic chips were discarded, and the metal shavings were retained in sealed polyethylene bags. Before dissolution, each sample was confirmed to be free of corrosion, inspected with a binocular microscope and scanning electron microscope (Hitachi TM3030Plus operating at 15 kV with an Oxford Instruments AZtec energy-dispersive spectrometer with the Oxford Instruments AZtecOne software platform). Approximately 100 mg of tin metal from each sample was digested in ultrapure concentrated HCl (12 M) heated at 100°C for 6 hours in enclosed Teflon containers.

A total of 17 cassiterite samples were analyzed: 11 single-crystal samples from the Pamirs of Pakistan and eastern Afghanistan and 6 samples from the Taurus region including 4 from Hisarcık and 2 from the Kestel mine. Cassiterite samples were digested following the procedure in (*49*): 0.25 g of −100-mesh cassiterite powder was mixed with 1 g of KCN and heated at 850°C for 1 hour in graphite crucibles contained within capped alumina crucibles. The resulting reduced tin metal beads were then dissolved in heated ultrapure 11 M HCl overnight.

Solutions were purified using the ion exchange chromatography described in (*50*). Samples were measured on the ThermoFinnigan Neptune multicollector inductively coupled plasma mass spectrometry (MC-ICPMS) at Peter Hooper GeoAnalytical Laboratory at the University of Washington, Pullman. The analytical procedure followed the methodology described in (*49*). Mass bias was corrected using Sb-doped solutions and an exponential mass bias correction defined in (*49*). The corrected values were bracketed with the National Institute of Standards and Technology (NIST) 3161A Sn standard (lot no. 07033) and data presented relative to this standard in per mil notation defined as

$$\delta^{124}\text{Sn‰} = \left(\frac{\left(\frac{^{124}\text{Sn}}{^{116}\text{Sn}}\right)\text{sample}}{\left(\frac{^{124}\text{Sn}}{^{116}\text{Sn}}\right)\text{ NIST 3161}} - 1 \right) \times 1000$$

Instrumentation 2σ error for δ^{124}Sn based on blocks of 25 analyses is ±0.02‰, and full procedural 2σ error is ±0.08‰ based on 10 measurements of an internal tin metal standard.

The new cassiterite values were added to published Sn isotopic analyses of cassiterite ores compiled from (*8*, *51*), with data from the latter being converted to equivalent NIST 3161 standardized $\delta^{124/116}$Sn values using the following equation: δ^{124}SnNIST 3161a = [$\delta^{124/120}$SnPuratronic × 2] + 0.26‰. Experimental studies by Berger *et al.* (*8*) documented a fractionating effect during smelting due to the evaporation of tin favoring the lighter isotopes. They suggest a +0.2‰ correction for the 8 atomic mass unit of δ^{124}Sn used here. Empirically, it was noted that the application of this +0.2‰ resulted in the best match between artifacts and ores in the Balkans (*8*). Accordingly, for comparison of the isotopic composition of cassiterite ores with that of the tin ingots, the δ^{124}Sn values of ores were reduced by 0.2‰.

Trace element concentrations were measured with a Thermo Fisher Scientific iCAP-Q at Rutgers University using a Teflon introduction system with 2% nitric acid with a trace of hydrofluoric acid in the carrier acid. Dwell times were 10 ms on each of the three channels, which were at 0.1 mass unit spacing from the peak center, and 10 runs were acquired for each sample and standard. Concentrations were determined by a five-point calibration using synthetic standard mixtures (High Purity Standard 68A-A, 68A-B, and 68A-C) that were doped with Sn to match the matrix of the samples. Precision was better than 2%.

Lead isotope analysis results of four Uluburun tin ingots (lot 9269, KW 0206, KW 1326, and KW 2699) were added to the dataset of 104 samples reported in (*6*). Lead purification was accomplished following the procedure derived from (*52*). Samples were measured on the Nu MC-ICPMS at the University of Florida. Mass bias was corrected using Tl-spiked samples similar to that described in (*53*). Standard NBS 981 was used, and 2σ errors of the standard were <0.001 for all ratios reported. Blind clustering of samples was conducted using *t*-SNE (*54*), a statistical method for dimensionality reduction. It is a nonlinear algorithm, unlike principal components analysis (*55*). *t*-SNE builds two separate probability-density functions capturing the similarity of each point in the dataset to each other point in the dataset, one for the full dimensionality data and another for the reduced dimensionality data. The locations of the points in the reduced dimensionality data are chosen to minimize the Kullback-Leibler divergence (*56*) between the two probability distributions. We used the Rtsne package implementation of the *t*-SNE algorithm, a base random number seed to ensure reproducibility, and ran the algorithm 1000 separate times (restarts), choosing the run with the lowest cost. The four inputs to the *t*-SNE algorithm were the isotopic ratios ^{206}Pb/^{204}Pb, ^{208}Pb/^{204}Pb, δ^{124}Sn, and the concentration of Pb with a perplexity of 30. Before running the *t*-SNE algorithm, we normalized each variable by subtracting the mean and dividing by the SD.

SUPPLEMENTARY MATERIALS

Supplementary material for this article is available at https://science.org/doi/10.1126/sciadv.abq3766

View/request a protocol for this paper from *Bio-protocol*.

REFERENCES AND NOTES

1. Z. Hu, S. Gao, Upper crustal abundances of trace elements: A revision and update. *Chem. Geol.* **253**, 205–221 (2008).
2. G. Barjamovic, Interlocking commercial networks and the infrastructure of trade in West Asia during the Bronze Age, in *Trade and Civilization in the Pre-Modern World*, K. Kristiansen, T. Lindkvist, J. Myrdal Eds. (Cambridge University Press, 2018), pp. 133–167.
3. S. Manning, P. Pulak, B. Kromer, S. Taiamo, C. Ramsey, M. Dee, Absolute Age of the Uluburun Shipwreck: A key late bronze age time-capsule for the east mediterranean, in *Tree-rings, Kings, and Old World Archaeology and Environment*, S. Manning, M. Bruce, Eds. (Oxford: Oxbow Books, 2009), pp. 163–188.
4. C. Pulak, The uluburun shipwreck: An overview. *Int. J. Naut. Archaeol.* **27**, 188–224 (1998).
5. C. Pulak, The Copper and Tin Ingots from the Late Bronze Age Shipwreck at Uluburun, in *International Symposium 'Anatolian Metal I'*, Ü. Yalçın, Der Anschnitt, Bochum, Beiheft Ed. (2000), vol. 13, pp. 137–157.
6. C. Pulak, The Uluburun tin ingots and the shipment of tin by sea in the Late Bronze Age Mediterranean. *TUBA-AR* **12**, 189–207 (2009).
7. W. Powell, M. Johnson, C. Pulak, K. A. Yener, R. Mathur, H. A. Bankoff, L. Godfrey, M. Price, E. Galili, From peaks to ports: Insights into tin provenance, production, and distribution from adapted applications of lead isotopic analysis of the Uluburun tin ingots. *J. Archaeol. Sci.* **134**, 105455 (2021).
8. D. Berger, E. Figueirdo, G. Brügmann, E. Pernicka, Tin isotope fractionation during experimental cassiterite smelting and its implication for tracing the tin sources of prehistoric metal artefacts. *J. Archaeol. Sci.* **92**, 73–86 (2018).

9. A. Mason, W. Powell, H. A. Bankoff, R. Mathur, M. Price, A. Bulatović, V. Filipović, Provenance of tin in the late bronze age balkans based on probabilistic and spatial analysis of Sn isotopes. *J. Archaeol. Sci.* **122**, 105181 (2020).
10. K. A. Yener, H. Özbal, E. Kaptan, A. N. Pehlivan, M. Goodway, Kestel: An early bronze age source of tin ore in the Taurus mountains, Turkey. *Science* **244**, 200–203 (1989).
11. J. Yao, R. Mathur, W. Powell, B. Lehmann, F. Tornos, M. Wilson, J. Ruiz, Sn-isotope fractionation as a record of hydrothermal redox reactions. *Am. Mineral.* **103**, 1591–1598 (2018).
12. D. L. Konopelko, R. I. Cherny, S. V. Petrov, S. Strekopytov, R. Seltmann, N. S. Vlasenko, V. V. Strekoptyov, Y. M. Mamadjanov, X.-S. Wang, O. Y. Plotinskaya, E. M. Andreeva, The Mushiston Sn deposit in Tajik Tien Shan as the type locality for stannite-cassiterite-hydrostannate mineralization: New mineral chemistry data and genetic constraints. *J. Geochem. Explor.* **239**, 107017 (2022).
13. O. P. Ivanov, L. Y. Yeremenko, A. I. Voronov, Y. M. Zorin, A. I. Kuzovenko, K. A. Khar'kevich, S. I. Kanoatov, Mineralogy and technology of new economic types of tin ores. *Int. Geol. Rev.* **35**, 603–612 (1993).
14. B. Reed, Descriptive model of porphyry Sn, in *Mineral Deposit Models*, D. Cox, D. Singer, Eds. (USGS Bulletin, 1986), p. 108.
15. W. Powell, R. Mathur, H. A. Bankoff, B. Kavur, M. Blečić-Kavur, Preliminary results of tin isotope analysis of LBA-EIA artifacts from Slovenia, Od Morja do Morja, Koper-Ptuj, Slovenia (2021).
16. R. Goldfarb, B. Berger, M. George, R. Seal II, Tellurium, in Critical mineral resources of the United States—Economic and environmental geology and prospects for future supply: U.S. Geological Survey Professional Paper 1802, K. J. Schulz, J. H. DeYoung Jr., R. R., Seal II, D. C. Bradley, Eds. (2017), pp. R1–R27; https://doi.org/10.3133/pp1802R.
17. F. Fayziev, A. Fayziev, M. Kayumarsi, On the silver mineralization of Central Tajikistan. *News of the Ural State Mining University* **4**, 18–22 (2017).
18. M. Smith, D. Banks, B. Yardley, A. Boyce, Fluid inclusion and stable isotope constraints on the genesis of the Cligga Head Sn-W deposit, S.W. England. *Eur. J. Mineral.* **8**, 961–974 (1996).
19. D. Berger, Q. Wang, G. Brügmann, N. Lockhoff, B. Roberts, E. Pernicka, The Salcombe metal cargoes: New light on the provenance and circulation of tin and copper in Later Bronze Age Europe provided by trace elements and isotopes. *J. Archaeol. Sci.* **138**, 105543 (2022).
20. S. Sabatini, Late Bronze Age oxhide and oxhide-like ingots from areas other than the Mediterranean: Problems and challenges. *Oxford J. Archaeol.* **35**, 29–45 (2016).
21. Z. Stos-Gale, "Biscuits with ears": A search for the origin of the earliest oxhide ingots, in *Metallurgy: Understanding How, Learning Why: Studies in Honor of James D. Muhly*, P. P. Betancourt, S. C. Ferrence, Eds. (INSTAP Academic Press, 2011), vol. 29.
22. N. Postgate, Bronze Age Bureaucracy. Writing and the Practice of Government in Assyria (Cambridge Univ. Press, 2013), p. 171.
23. J. Thomalsky, Afghanistan. Ancient mining and metallurgy. Initial project stage, in *Proceedings of the 9th International Congress on the Archaeology of the Ancient Near East, 9th ICAANE*, R. A. Stucky, O. Kaelin, H.-P. Mathys, Eds. (Wiesbaden, 2016), pp. 647–661.
24. N. Nezafati, E. Pernicka, M. Momenzadeh, Early tin-copper ore from Iran, a possible clue for the enigma of Bronze Age Tin, in Ü. Yalçin (ed.), *Anatolian Metal V*, Der Anschnitt 24, Bochum (2011), pp. 211–230.
25. T. Stöllner, Z. Samaschev, S. Berdenov J. Cierny, M. Doll, J. Garner, A. Gontscharov, A. Gorelik, A. Hauptmann, R. Herd, G. A. Kusch, V. Merz, T. Riese, B. Sikorski, B. Zickgraf, Tin from Kazakhstan - Steppe Tin for the West?, in Anatolian Metal. V: Beiträge des im November 2008 in Bochum veranstalteten Internationalen Symposiums "Anatolian Metal V," Veröffentlichungen aus dem Deutschen Bergbau-Museum Bochum, Nr. (2011), vol. 180, pp. 231–252.
26. J. Garner, Das Zinn der Bronzezeit in Mittelasien II. Die Montanarchaeologischen Forschungen an den Zinn Lagerstätten. Archäologie in Iran and Turan 12. Berlin: Deutsches Archäologisches Institut, Bochum: Deutsches Bergbau-Museums (2013).
27. K. A. Yener, F. Kulakoğlu, E. Yazgan, R. Kontani, Y. S. Hayakawa, J. W. Lehner, G. Dardeniz, G. Öztürk, M. Johnson, E. Kaptan, A. Hacar, New tin mines and production sites near Kültepe in Turkey: A third-millennium BC highland production model. *Antiquity* **89**, 596–612 (2015).
28. K. A. Yener, Göltepe Excavations: Tin Production at an Early Bronze Age Mining Town in the Central Taurus Mountains, Turkey (INSTAP Academic Press, 2021).
29. J. F. Tolksdorf, F. Schröder, L. Petr, C. Herbig, K. Kaiser, P. Kočár, C. Hemker, Evidence for bronze age and medieval tin placer mining in the Erzgebirge mountains, Saxony (Germany). *Geoarchaeology* **35**, 198–216 (2020).
30. A. Huska, W. Powell, S. Mitrović, H. A. Bankoff, A. Bulatović, V. Filipović, R. Boger, Placer tin ores from Mt. Cer, West Serbia, and their potential exploitation during the bronze age. *Geoarchaeology* **29**, 477–493 (2014).
31. H. Parzinger, N. Boroffka, Das Zinn der Bronzezeit in Mittelasien I. Archäologie in Iran und Turan 5, Mainz am Rhein: Philipp von Zabern (2003).
32. J. Bendezu-Sarmiento, J. Lhuillier, La Protohistoria en Asia Central, entre las edades del Bronce y del Hierro. Nuevas investigaciones arqueológicas entre el Uzbekistán y el Turkmenistán. A. J. Domínguez Monedero, C. del Cerro Linares, F. J. Villalba Ruiz de Toledo, F. L. Borrego Gallardo Nomina in Aqua Scripta. Homenaje a Joaquin Maria Cordoba Zoilo, 978-84-8344-762-8 (2021).
33. N. M. Vinogradova, E. E. Kuz'mina, Contacts between the steppe and agricultural tribes of Central Asia in the Bronze Age. *Anthropology and Archaeology of Eurasia* **34**, 29–54 (1996).
34. M. Frachetti, Multiregional emergence of mobile pastoralism and nonuniform institutional complexity across Eurasia. *Curr. Anthropol.* **53**, 2–38 (2012).
35. X. Zhou, J. Yu, R. Spengler, H. Shen, K. Zhao, J. Ge, Y. Bao, J. Liu, Q. Yang, G. Chen, P. Jia, X. Li, 5,200-year-old cereal grains from the Eastern Altai Mountains redate the trans-eurasian crop exchange. *Nat. Plants* **6**, 78–87 (2020).
36. Y. Li, Agriculture and palaeoeconomy in prehistoric Xinjiang, China (3000-200 BC). *Veg. Hist. Archaeobotany* **30**, 287–303 (2021).
37. G. M. Matuzeviciute, T. Kubatbek, T. Hermes, E. Ananyevskaya, M. Grikpedis, E. Luneau, I. Merkyte, L. Rouse, High-altitude agro-pastoralism in the Kyrgyz Tien Shan: New excavations of the Chap Farmstead (1065–825 cal b.c.). *J. Field Archaeol.* **45**, 29–45 (2020).
38. P. D. Dupuy, E. Luneau, L. Rouse, Pluralising power: Ceramics and social differentiation in Bronze Age central Eurasia. *World Archaeol.* 779–808 (2021).
39. M. Wagner, M. Hallgren-Brekenkamp, D. Xu, X. Kang, P. Wertmann, C. James, I. Elkina, D. Hosner, C. Leipe, P. Tarasov, The invention of twill tapestry points to Central Asia: Archaeological record of multiple textile techniques used to make the woollen outfit of a ca. 3000-year-old horse rider from Turfan, China. *Archaeol. Res. Asia* **29**, 100344 (2022).
40. R. Spengler, M. D. Frachetti, P. N. Domani, Late Bronze Age agriculture at Tasbas in the Dzhungar Mountains of eastern Kazakhstan. *Quat. Int.* **348**, 147–157 (2014).
41. V. C. Pigott, The Bactria-Margiana Archaeological Complex (BMAC), the Seima-Turbino Horizon and A Possible Eastward Transmission of Tin-Bronze Technology Through Later Third Millennium BCE Central Asia to the Altai Mountains/Eastern Steppe, in *How Objects Tell Stories: Essays in Honor of Emma C. Bunker, Inner and Central Asian Art and Archaeology 1*, K. M. Linduff, K. S. Rubinson, Eds. (Turnhout: Brepols, 2018), pp. 191–121.
42. P. de Barros Damgaard, R. Martiniano, J. Kamm, J. V. Moreno-Mayar, G. Kroonen, M. Peyrot, G. Barjamovic, S. Rasmussen, C. Zacho, N. Baimukhanov, V. Zaibert, V. Merz, A. Biddanda, I. Merz, V. Loman, V. Evdokimov, E. Usmanova, B. Hemphill, A. Seguin-Orlando, F. E. Yediay, I. Ullah, K.-G. Sjögren, K. H. Iversen, J. Choin, C. de la Fuente, M. Ilardo, H. Schroeder, V. Moiseyev, A. Gromov, A. Polyakov, S. Omura, S. Y. Senyurt, H. Ahmad, C. M. Kenzie, A. Margaryan, A. Hameed, A. Samad, N. Gul, M. H. Khokhar, O. I. Goriunova, V. I. Bazaliiskii, J. Novembre, A. W. Weber, L. Orlando, M. E. Allentoft, R. Nielsen, K. Kristiansen, M. Sikora, A. K. Outram, R. Durbin, E. Willerslev, The first horse herders and the impact of early Bronze Age steppe expansions into Asia. *Science* **360**, eaar7711 (2018).
43. V. M. Narasimhan, N. Patterson, P. Moorjani, N. Rohland, R. Bernardos, S. Mallick, I. Lazaridis, N. Nakatsuka, I. Olalde, M. Lipson, A. M. Kim, L. M. Olivieri, A. Coppa, M. Vidale, J. Mallory, V. Moiseyev, E. Kitov, J. Monge, N. Adamski, N. Alex, N. Broomandkhoshbacht, F. Candilio, K. Callan, O. Cheronet, B. J. Culleton, M. Ferry, D. Fernandes, S. Freilich, B. Gamarra, D. Gaudio, M. Hajdinjak, É. Harney, T. K. Harper, D. Keating, A. M. Lawson, M. Mah, K. Mandl, M. Michel, M. Novak, J. Oppenheimer, N. Rai, K. Sirak, V. Slon, K. Stewardson, F. Zalzala, Z. Zhang, G. Akhatov, A. N. Bagashev, A. Bagnera, B. Baitanayev, J. Bendezu-Sarmiento, A. A. Bissembaev, G. L. Bonora, T. T. Chargynov, T. Chikisheva, P. K. Dashkovskiy, A. Derevianko, M. Dobeš, K. Douka, N. Dubova, M. N. Duisengali, D. Enshin, A. Epimakhov, A. V. Fribus, D. Fuller, A. Goryachev, A. Gromov, S. P. Grushin, B. Hanks, M. Judd, E. Kazizov, A. Khokhlov, A. P. Krygin, E. Kupriyanova, P. Kuznetsov, D. Luiselli, F. Maksudov, A. M. Mamedov, T. B. Mamirov, C. Meiklejohn, D. C. Merrett, R. Micheli, O. Mochalov, S. Mustafokulov, A. Nayak, D. Pettener, R. Potts, D. Razhev, M. Rykun, S. Sarno, T. M. Savenkova, K. Sikhymbaeva, S. M. Slepchenko, O. A. Soltobaev, N. Stepanova, S. Svyatko, K. Tabaldiev, M. Teschler-Nicola, A. A. Tishkin, V. V. Tkachev, S. Vasilyev, P. Velemínský, D. Voyakin, A. Yermolayeva, M. Zahir, V. S. Zubkov, A. Zubova, V. S. Shinde, C. Lalueza-Fox, M. Meyer, D. Anthony, N. Boivin, K. Thangaraj, D. J. Kennett, M. Frachetti, R. Pinhasi, D. Reich, The formation of human populations in South and Central Asia. *Science* **365**, eaat7487 (2019).
44. T. Hermes, P. D. Dupuy, E. Henry, M. Meyer, A. Mar'yashev, M. Frachetti, The multi-period settlement Dali in Southeastern Kazakhstan: Bronze age institutional dynamics along the inner asian mountain corridor. *Asian Perspectives* **60**, 345–381 (2021).
45. V. C. Pigott, The acquisition of tin in bronze age Southwest Asia, in *The World of the Oxus Civilization*, B. Lyonnet, N. A. Dubova, Eds. (Routledge, 2020), pp. 827–861.
46. S. Campbell, J. Moon, R. Killick, D. Calderbank, E. Robson, M. Shepperson, F. Slater, Tell Khaiber: An administrative centre of the Sealand period. *Iraq* **79**, 21–46 (2017).
47. S. Laursen, P. Steinkeller, *Babylonia, the Gulf Region, and the Indus Archaeological and Textual Evidence for Contact in the Third and Early Second Millennium BC* (Eisenbrauns, 2017).
48. S. Košak, Hittite inventory texts (CTH 241-250). Heidelberg: Carl Winter Universitätsverlag.49 S. Siegelova, H. Tsumoto, 2011. Metals and Metallurgy in Hittite

Anatolia, in *Insights into Hittite History and Archaeology*, H. Genz, D. P. Mielke, Eds. (Peeters, 1982), pp. 275–300.
49. R. Mathur, W. Powell, A. Mason, L. Godfrey, J. Yao, M. E. Baker, Preparation and measurement of cassiterite for Sn isotope analysis. *Geostand. Geoanal. Res.* **41**, 701–707 (2017).
50. E. Balliana, M. Aramendía, M. Resano, C. Barbante, F. Vanhaecke, Copper and tin isotopic analysis of ancient bronzes for archaeological investigation: Development and validation of a suitable analytical methodology. *Anal. Bioanal. Chem.* **405**, 2973–2986 (2013).
51. D. Berger, J. Soles, A. Giumlia-Mair, G. Brügmann, E. Galili, N. Lockhoff, E. Pernicka, Isotope systematics and chemical composition of tin ingots from Mochlos (Crete) and other Late Bronze Age sites in the eastern Mediterranean Sea: An ultimate key to tin provenance? *PLOS ONE* **14**, e0218326 (2019).
52. A. M. Thibodeau, J. T. Chesley, J. Ruiz, Lead isotope analysis as a new method for identifying material culture belonging to the Vázquez de Coronado expedition. *J. Archaeol. Sci.* **39**, 58–66 (2012).
53. G. Kamenov, P. Mueller, M. Perfit, Optimization of mixed Pb–Tl solutions for high precision isotopic analyses by MC-ICP-MS. *J. Anal. At. Spectrom* **19**, 1262–1267 (2004).
54. J. Krijthe, Rtsne: T-distributed stochastic neighbor embedding using Barnes-Hut implementation (2015); https://github.com/jkrijthe/Rtsne.
55. C. Aggarwal, Data mining: The textbook (Springer, 2015), p. 763.
56. S. Hoque, D. MacKay, *Information Theory, Inference and Learning Algorithms* (Cambridge Univ. Press, 2003), p. 640.

Acknowledgments: We acknowledge J. Vervoort for making the Washington State University facility available. We thank L. Godfrey for the use of and assistance in operation of the mass spectrometer at Rutgers University. We are indebted to H. Özbal, Boğaziçi (Bosphorus) University, Istanbul, Turkey for providing a sample of Bolkardağ ore for isotopic analysis. **Funding:** The project was funded in part by Professional Staff Congress-City University of New York Research Award TRADB-50-249, in addition to a research grant from the Institute for the Aegean Prehistory, and Professional Staff Congress-City University of New York Research Award TRADB-50-249 Institute for Aegean Prehistory Research Grant. **Author contributions:** Conceptualization: W.P. Methodology: W.P. and R.M. Provision of samples: C.P. Investigation: W.P. and R.M. Programming: M.P. Statistical analysis: M.P. Visualization: W.P. and M.F. Funding acquisition: W.P. Project administration: W.P. and M.F. Writing—original draft: W.P., M.F., C.P., H.A.B., G.B., M.J., R.M., V.C.P., M.P., and K.A.Y. Writing—review and editing: W.P., M.F., C.P., H.A.B., G.B., M.J., R.M., V.C.P., M.P., and K.A.Y. **Competing interests:** The authors declare that they have no competing interests. **Data and materials availability:** All data needed to evaluate the conclusions in the paper are present in the paper and/or the Supplementary Materials. The R code and data are freely available for download at https://zenodo.org/record/7072821 (DOI: 10.5281/zenodo.7072821) and archived at https://github.com/MichaelHoltonPrice/uluburun_tsne.

Submitted 4 April 2022
Accepted 14 September 2022
Published 30 November 2022
10.1126/sciadv.abq3766

Science Advances

Supplementary Materials for

Tin from Uluburun shipwreck shows small-scale commodity exchange fueled continental tin supply across Late Bronze Age Eurasia

Wayne Powell *et al.*

Corresponding author: Wayne Powell, wpowell@brooklyn.cuny.edu; Michael Frachetti, frachetti@wustl.edu

Sci. Adv. **8**, eabq3766 (2022)
DOI: 10.1126/sciadv.abq3766

This PDF file includes:

Table S1
Fig. S1

Table S1. Isotopic and trace element analyses of Uluburun tin ingots.

Museum #	Group	Form	Fraction	206/204	207/204	208/204	124/116	Mn	Co	Ni	Cu	Zn	As	Nb	Ag	Cd	In	Sb	Te	Ta	W	Au	Pb	Bi	U
KW 0022	P1	Fragment	Fragment	19.654	15.663	38.438	0.61	12.9	8.87	8.9	170.9	130.8	35.1	0.02	0.71	0.44	28.7	9.8	0.00	0.01	1.40	0.07	35.0	49.0	0.03
KW 0035	MC1A	Oxhide	¼	19.049	15.697	38.979	1.24	27.7	6.04	43.2	94.5	218.9	24.8	0.04	0.68	0.87	31.8	8.7	0.00	0.00	1.11	0.08	169.6	56.4	0.02
KW 0095	MC1C	Oxhide	¼	19.005	15.727	39.086	-0.15	18.5	5.64	12.6	96.9	140.7	38.9	0.03	1.12	0.33	29.9	7.9	0.00	0.01	1.13	0.07	663.7	52.3	0.02
KW 0110	MC2A	Oxhide	¼	18.852	15.616	38.791	0.84	10.2	6.27	14.8	263.6	184.4	23.7	0.01	8.31	0.22	35.6	20.9	5.86	0.00	0.86	0.07	1640.0	60.7	0.01
KW 0133	P2A	Oxhide	¼	18.889	15.662	38.641	0.14	1305.5	6.33	24.8	361.3	552.8	15.6	0.03	0.70	1.15	28.3	12.7	0.00	0.01	1.06	3.43	91.5	52.6	0.02
KW 0197	MC1A	Slab Thin	Full	18.970	15.720	39.022	0.68	72.6	5.75	48.9	702.7	143.3	49.4	0.04	1.80	0.60	25.6	21.2	2.64	0.01	1.46	0.89	271.3	56.4	0.02
KW 0198	MC2A	Slab	¼	18.829	15.686	38.813	0.64	118.4	6.55	31.0	10906.9	352.2	121.0	0.03	1.87	1.11	26.3	21.0	0.00	0.01	1.08	0.38	1107.8	35.9	0.01
KW 0199	MC1A	Bun	Full	18.743	15.704	38.937	0.58	445.5	10.58	103.1	10283.9	162.0	54.2	0.05	80.96	1.31	12.0	1349.3	6.63	0.01	6.13	0.26	115234.7	101.5	0.27
KW 0201	MC1A	Slab	¼	18.983	15.758	39.177	0.83	31.4	6.93	27.6	1098.6	547.9	51.7	0.02	4.38	0.57	25.5	11.1	0.00	0.01	0.82	0.76	2588.2	50.0	0.02
KW 0204	MC1B	Oxhide	¼	19.225	15.748	38.931	0.73	25.5	5.97	21.0	150.0	265.0	38.3	0.03	0.50	0.52	27.7	6.6	0.00	0.01	1.38	0.15	45.4	39.3	0.04
KW 0205	MC1A	Oxhide	¼	18.980	15.727	39.076	1.13	20.3	6.16	14.4	127.7	148.8	34.9	0.01	7.27	0.19	30.1	11.6	0.69	0.01	13.63	0.09	1363.1	54.3	0.01
KW 0206	P1	Oxhide	¼	18.812	15.654	38.521	0.87	26.0	6.17	25.9	1330.2	420.0	63.5	0.04	1.77	1.10	22.8	22.3	0.00	0.01	6.56	4.34	116.6	32.6	0.02
KW 0241	MC1A	Slab	¼	18.894	15.707	38.889	0.77	21.6	5.92	22.9	240.7	510.8	42.5	0.03	3.62	0.83	27.1	8.0	0.88	0.01	1.39	0.87	5013.4	45.2	0.03
KW 0242	MC1A	Slab	¼	18.907	15.701	38.921	0.86	61.8	6.01	24.8	113.4	490.4	37.2	0.03	1.59	28.26	22.8	12.8	4.00	0.01	1.06	0.34	1154.8	32.1	0.02
KW 0243	MC2A	Slab	¼	18.829	15.688	38.814	1.03	29.0	10.07	38.4	1227.3	685.6	35.6	0.06	2.39	1.64	29.0	32.6	5.57	0.01	8.52	0.24	1173.4	35.7	0.02
KW 0244	MC1A	Slab	½	18.956	15.679	38.973	1.10	84.3	6.71	34.5	230.6	369.0	32.5	0.03	10.01	1.15	29.8	17.7	7.45	0.01	1.01	0.30	1410.7	51.8	0.02
KW 0245	MC1A	Slab Thin	¼	18.918	15.719	38.982	0.61	59.4	7.92	44.3	486.3	673.0	33.6	0.05	9.99	2.04	37.7	21.8	7.10	0.00	1.03	0.34	13756.8	64.5	0.01
KW 0315	MC1A	Oxhide	¼	18.994	15.699	39.028	0.42	79.1	7.31	39.2	232.5	381.8	23.4	0.03	18.71	1.15	30.8	63.7	3.24	0.01	1.45	0.15	9517.0	46.6	0.02
KW 0341	P2A	Oxhide	Ear	18.771	15.581	38.262	0.09	858.2	8.04	37.4	150.0	2833.5	49.2	0.02	12.44	1.64	42.8	33.2	17.18	0.00	0.60	0.07	1316.7	72.6	0.01
KW 0391	MC1A	Oxhide	¼	18.967	15.735	38.960	1.12	22.7	9.01	96.1	3013.7	136.0	62.6	0.02	1.40	0.46	38.8	13.4	1.45	0.01	1.17	0.09	155.3	63.6	0.02
KW 0392	MC1A	Slab	¼	18.912	15.712	38.953	0.97	9.1	6.15	50.9	203.2	232.8	28.7	0.04	2.21	0.46	27.0	13.5	0.00	0.03	1.39	4.42	2071.5	50.0	0.02
KW 0393	MC1A	Slab	½	18.905	15.704	38.934	0.50	15.5	6.20	15.2	2318.2	263.4	24.8	0.01	5.55	0.47	27.7	19.9	4.40	0.01	1.39	0.86	6096.4	57.2	0.01
KW 0398	P1	Oxhide	¼	19.741	15.733	38.590	0.80	31.7	6.39	85.7	159.2	451.7	26.6	0.11	0.87	0.80	28.7	9.8	0.00	0.01	1.30	0.46	40.1	38.1	0.08
KW 0399	P1	Oxhide	¼	18.949	15.664	38.500	0.83	11.5	5.83	4.9	124.6	35.4	18.7	0.01	0.44	0.07	21.8	3.4	0.00	0.00	0.40	0.01	34.7	24.2	0.00
KW 0400	P1	Oxhide	¼	20.160	15.752	38.598	0.84	25.3	7.35	127.2	419.4	690.8	27.4	0.03	0.85	1.51	36.4	15.2	5.51	0.01	2.20	0.20	106.3	68.6	0.02
KW 0401	MC1A	Bun	Full	19.009	15.706	38.984	0.84	13.9	6.11	15.3	114.4	282.9	22.7	0.01	0.92	0.72	28.6	12.2	0.67	0.01	1.09	0.17	277.8	56.3	0.01
KW 0403	Unknown	Oxhide	¼	19.026	16.146	39.079	0.69	13.3	6.28	11.9	156.2	196.3	23.3	0.01	0.55	0.42	36.5	10.1	0.49	0.01	1.44	0.19	68.3	56.1	0.01
KW 0412	P2A	Slab	½	18.669	15.531	38.213	0.19	126.8	7.52	32.2	2369.8	119.6	17.1	0.03	5.72	0.72	31.1	34.0	15.40	0.01	1.04	0.13	5522.8	71.5	0.02
KW 0511	P1	Oxhide	¼	18.815	15.656	38.495	0.75	18.2	6.46	13.9	154.0	260.7	24.3	0.02	0.62	0.53	35.4	12.7	4.88	0.01	0.67	0.09	77.5	53.7	0.02
KW 0515	P1	Oxhide	¼	19.316	15.678	38.593	0.97	87.3	6.23	46.6	224.5	373.0	25.6	0.03	1.41	5.66	27.1	15.9	0.73	0.01	1.18	4.47	48.2	47.7	0.01
KW 0516	Unknown	Oxhide	¼	19.580	15.551	37.565	-0.88	4279.3	7.67	19.9	244.3	1767.4	13.1	0.01	0.50	6.92	34.8	15.6	5.23	0.00	0.75	0.76	161.6	58.2	0.01
KW 0518a	MC1A	Slab	¼	18.830	15.684	38.847	0.52	110.8	6.85	24.1	176.1	181.2	7.4	0.04	0.94	0.40	30.0	22.4	1.25	0.02	0.59	0.48	1143.9	36.6	0.01
KW 0518b	MC1C	Slab	¼	18.832	15.692	38.861	-0.27	67.9	8.11	32.6	551.7	201.0	8.3	0.01	1.59	0.51	39.5	36.5	15.86	0.00	0.59	0.22	877.4	42.1	0.02
KW 0519	MC1A	Bun	½	18.900	15.703	38.960	0.79	24.3	7.22	41.2	1130.7	303.7	26.6	0.03	6.13	0.85	33.5	24.2	5.00	0.01	1.19	0.63	4671.1	45.4	0.01
KW 0633	MC1A	Oxhide	¼	19.003	15.709	38.979	0.90	37.8	6.31	12.9	112.7	162.5	21.8	0.01	3.79	0.26	28.6	14.3	2.90	0.01	1.11	0.21	371.1	47.9	0.02
KW 0637	P1	Oxhide	¼	19.654	15.663	38.438	0.52	16.1	7.32	24.9	99.0	390.5	21.3	0.02	0.63	1.10	31.0	18.9	9.12	0.01	0.94	0.14	37.9	42.4	0.02
KW 0638	MC1A	Oxhide	¼	19.017	15.721	39.032	0.64	22.9	7.32	21.8	107.7	371.0	24.8	0.13	4.21	1.17	31.2	17.3	6.68	0.34	1.60	0.19	243.6	52.3	0.07
KW 0639a	MC1C	Oxhide	¼	18.950	15.694	38.993	-0.70	3197.7	9.53	43.6	2606.5	545.3	17.7	0.01	8.33	2.34	40.0	35.1	15.40	0.00	6.62	0.05	1480.8	54.3	0.01
KW 0640	MC1A	Oxhide	½	19.010	15.744	39.153	0.59	61.7	6.21	20.0	98.9	280.3	19.4	0.01	1.39	0.97	24.4	42.8	4.84	0.01	1.19	0.09	1870.0	36.9	0.01
KW 0641a	MC2B	Oxhide	¼	19.210	15.702	38.767	0.61	66.0	6.52	22.9	96.2	568.2	20.0	0.04	3.64	1.62	25.2	19.0	2.26	0.02	1.10	5.28	518.8	46.5	0.02
KW 0642	MC1A	Bun	½	18.934	15.680	38.936	0.51	23.4	6.62	15.5	361.3	212.1	18.6	0.02	1.23	0.86	29.8	14.4	2.69	0.01	1.06	1.06	225.3	57.0	0.01
KW 0643	MC1A	Oxhide	¼	18.998	15.703	39.024	0.33	42.3	6.67	31.7	114.6	320.7	19.1	0.05	3.51	0.81	27.7	20.9	5.34	0.01	1.05	0.60	814.2	53.1	0.01
KW 0644	MC2A	Oxhide	½	18.680	15.712	38.773	0.77	18.7	5.71	17.5	132.2	439.9	20.7	0.02	0.69	1.13	24.6	13.0	0.00	0.01	0.71	0.45	693.5	45.1	0.01
KW 0702	P2A	Oxhide	¼	18.871	15.638	38.572	0.17	144.8	6.18	17.4	134.8	689.3	7.5	0.01	0.47	0.39	27.6	10.2	0.00	0.00	0.58	0.25	91.3	47.1	0.01
KW 0704	MC1A	Slab	Fragment	18.985	15.707	39.038	0.42	13.1	6.31	16.2	1511.5	276.6	19.3	0.02	2.84	0.48	22.0	21.1	1.10	0.08	0.84	0.92	2735.7	50.2	0.04
KW 0712	MC2A	Oxhide	¼	19.205	15.701	38.767	1.07	44.3	6.38	15.4	193.6	288.0	20.6	2.85	0.65	0.83	31.0	11.6	0.00	2.11	1.29	0.33	49.9	43.0	0.11
KW 0718	MC2A	Oxhide	¼	18.936	15.664	38.719	0.84	24.5	6.68	18.3	151.6	387.7	20.5	0.03	1.24	1.97	30.7	13.3	0.26	0.01	7.90	0.32	131.6	58.4	0.02
KW 0719	MC1A	Slab	¼	18.966	15.727	39.054	0.42	30.8	7.76	57.5	1244.3	249.0	15.8	0.04	4.65	0.44	33.1	21.7	7.11	0.00	0.75	0.87	2972.3	59.9	0.01
KW 0720	MC1A	Unique	Full	19.038	15.750	39.155	1.20	18.6	6.09	25.9	124.7	204.8	18.9	0.02	0.95	0.86	26.3	10.1	0.00	0.01	0.84	0.30	231.4	48.9	0.01
KW 0721	MC2A	Oxhide	¼	18.950	15.684	38.793	0.80	301.9	7.50	22.2	170.2	497.9	25.7	0.02	0.97	1.45	39.0	14.2	5.44	0.01	1.64	5.25	152.1	69.8	0.01
KW 0722	P2A	Oxhide	¼	18.940	15.663	38.717	0.13	14.1	6.51	16.1	1510.6	270.8	22.9	0.02	4.84	0.75	30.3	18.4	6.75	0.01	1.88	1.05	234.8	50.3	0.02
KW 0847	MC1A	Bun	⅓	18.874	15.695	38.886	0.54	63.4	7.57	48.1	1556.7	409.8	37.7	0.05	32.56	1.01	24.1	101.0	2.77	0.04	5.65	0.58	58802.3	63.3	0.02
KW 0946	MC1A	Slab	¼	18.927	15.716	39.012	0.73	29.2	7.01	19.5	466.2	158.7	22.1	0.02	8.78	0.61	38.6	20.2	6.49	0.01	1.11	1.00	3987.4	70.8	0.01
KW 1321	MC1C	Oxhide	¼	18.975	15.690	38.878	-0.54	18.2	7.50	43.2	191.5	351.0	8.9	0.03	0.56	0.52	32.2	15.6	5.24	0.01	0.65	0.27	106.6	66.0	0.01

KW 1326	MC1A	Bun	Fragment	18.991	15.689	39.034	0.88	26.4	6.52	17.4	1675.1	182.6	40.3	0.01	#####	0.55	24.1	244.9	0.00	0.01	1.02	0.30	130101.8	109.9	0.05
KW 1357	MC1C	Oxhide	¼	19.748	15.738	38.820	-0.31	8.2	6.06	11.1	105.8	146.4	8.9	0.01	0.32	0.22	27.1	13.5	0.29	0.00	0.30	0.21	22.0	47.3	0.01
KW 1371	MC1A	Oxhide	½	19.030	15.728	39.075	0.50	14.5	6.72	12.4	134.1	157.4	25.8	0.01	0.95	0.32	35.2	16.5	8.25	0.01	1.29	0.16	463.1	60.8	0.02
KW 1760	P1	Fragment	Fragment	19.647	15.726	38.633	0.61	36.8	6.99	38.1	106.7	365.5	25.2	0.01	0.56	0.79	33.4	19.3	10.51	0.01	0.71	0.10	42.5	44.5	0.01
KW 1932	P1	Oxhide	Full	19.288	15.669	38.405	0.62	31.6	6.19	14.3	114.5	166.9	21.7	0.04	0.48	0.45	31.8	14.0	4.51	0.02	0.93	0.11	36.4	47.9	0.02
KW 2143	P1	Oxhide	¼	19.890	15.777	38.713	0.78	20.5	5.96	12.8	88.0	231.0	17.8	0.02	0.43	0.50	29.3	15.8	1.87	0.01	1.35	5.51	33.1	38.5	0.01
KW 2255	P1	Oxhide	¼	19.637	15.707	38.522	1.22	3114.5	6.82	13.9	160.2	666.3	25.2	0.02	0.47	1.49	29.8	12.6	1.50	0.01	1.60	1.08	36.8	38.0	0.02
KW 2329	P2B	Wedge	Full	19.919	15.591	38.137	0.29	394.0	7.89	42.7	534.3	175.7	10.7	0.01	2.86	1.41	46.2	23.9	17.33	0.00	1.83	0.31	48.3	65.6	0.01
KW 2332	P2B	Wedge	Full	19.758	15.755	38.741	0.40	20.3	6.76	18.8	410.7	1349.9	18.2	0.02	0.56	0.52	32.1	18.4	5.83	0.03	1.11	0.36	33.2	55.1	0.01
KW 2365	P2B	Wedge	Full	20.037	15.727	38.543	0.01	44.8	7.68	45.1	552.8	451.0	18.5	0.04	0.80	3.49	33.6	19.4	4.73	0.01	1.54	0.28	102.3	58.6	0.01
KW 2408	MC1B	Oxhide	¼	19.869	15.797	38.863	0.82	52.2	7.63	75.2	211.9	297.8	18.3	0.06	0.56	1.74	31.0	22.4	9.44	0.01	1.53	0.22	49.8	37.6	0.01
KW 2699	MC1A	Slab Thin	¼	19.006	15.693	39.045	0.54	310.3	8.71	35.3	1154.7	213.8	8.5	0.03	1.49	2.11	31.9	21.0	7.25	0.00	0.83	0.18	1600.7	59.6	0.03
KW 2739	P1	Oxhide	¼	19.634	15.726	38.648	0.92	1620.1	7.91	25.0	267.9	718.7	23.0	0.03	1.07	1.93	37.9	13.1	6.94	0.01	1.66	0.18	62.3	65.5	0.02
KW 2774	MC1A	Oxhide	¼	19.019	15.738	39.143	0.25	58.3	6.95	32.2	123.0	506.3	13.9	0.04	2.27	1.01	23.8	31.8	0.29	0.01	1.06	0.16	830.3	48.3	0.01
KW 2777	MC2A	Oxhide	¼	18.659	15.665	38.751	0.70	5379.0	8.65	23.6	837.2	1266.7	18.7	0.08	0.64	3.28	39.4	20.0	14.50	0.05	12.52	0.10	45.3	52.0	0.01
KW 2789	P1	Oxhide	¼	19.760	15.719	38.563	1.05	202.6	6.92	59.9	197.6	371.7	36.6	0.06	15.17	0.75	32.3	13.1	1.53	0.03	16.77	5.60	38.9	50.7	0.03
KW 2796	P1	Oxhide	¼	19.781	15.709	38.517	0.81	24.4	6.05	12.9	187.0	151.3	27.8	0.04	0.52	0.27	29.6	12.3	0.00	0.01	8.76	1.09	38.5	45.8	0.01
KW 2874	MC1C	Oxhide	¼	18.953	15.670	38.861	-0.17	845.2	18.47	680.9	5829.2	270.0	32.8	0.56	3.07	1.55	41.9	36.2	13.41	0.01	7.86	0.31	580.9	62.6	0.02
KW 2887	P2A	Oxhide	¼	18.993	15.639	38.405	-0.45	4609.3	7.75	26.5	588.3	803.9	11.6	0.04	0.73	3.32	31.3	17.3	3.31	0.02	31.69	0.40	68.1	52.9	0.02
KW 2902	MC1A	Oxhide	¼	19.005	15.716	38.971	0.24	13.3	7.34	20.9	112.7	391.2	28.1	0.04	1.13	0.60	26.4	24.4	3.58	0.02	6.61	0.33	90.7	68.3	0.02
KW 2911	MC1A	Slab	Full	19.009	15.785	39.260	0.31	36.5	7.53	27.1	3058.7	328.9	23.3	0.03	16.86	0.42	30.6	58.7	6.95	0.02	5.27	0.36	11458.9	54.2	0.02
KW 2915	MC1A	Slab	Full	18.990	15.702	39.018	0.67	14.2	4.76	2.1	1650.0	159.8	21.7	0.11	9.88	0.26	18.0	19.9	0.00	0.03	23.18	0.26	3155.6	28.8	0.01
KW 2922	MC2B	Oxhide	Full	19.347	15.706	38.769	0.70	22.4	6.67	22.5	137.2	182.8	21.3	0.06	0.57	0.32	33.4	16.0	4.70	0.03	5.26	0.20	54.9	54.3	0.03
KW 2924	P1	Oxhide	Full	18.784	15.652	38.378	0.86	13.7	6.32	16.9	219.2	210.3	18.9	0.03	0.63	0.65	32.8	10.3	0.00	0.01	34.37	0.19	78.1	56.5	0.01
KW 3014	P1	Oxhide	¼	19.164	15.690	38.546	0.77	26.9	6.73	20.1	137.2	423.0	18.0	0.03	0.52	0.58	32.9	13.8	1.68	0.01	3.03	0.15	37.9	62.0	0.01
KW 3048	P1	Oxhide	¼	19.166	15.679	38.457	0.70	679.6	7.24	20.1	106.1	315.6	16.7	0.03	3.10	0.57	32.0	31.7	6.84	0.03	2.82	6.85	2185.8	49.1	0.03
KW 3061	P1	Oxhide	¼	19.759	15.729	38.502	0.72	12.3	6.77	14.9	91.2	187.4	17.1	0.03	0.45	0.35	34.0	15.7	4.86	0.02	5.76	1.64	30.4	50.0	0.01
KW 3094	MC1A	Oxhide	¼	19.082	15.695	38.920	0.94	89.0	6.42	37.3	142.3	162.4	19.2	0.03	0.45	0.48	28.3	14.5	2.11	0.05	3.83	0.93	96.0	51.0	0.01
KW 3157	MC2A	Oxhide	¼	19.047	15.698	38.778	0.80	90.0	8.02	49.2	987.5	123.3	22.5	0.05	1.54	0.52	52.1	19.4	10.58	0.01	14.50	0.51	75.9	81.6	0.02
KW 3297	MC1A	Oxhide	½	19.019	15.690	38.959	0.89	23.6	6.78	13.2	100.7	198.9	21.1	0.03	0.63	0.44	32.7	17.3	6.68	0.03	1.82	0.46	271.2	55.0	0.01
KW 3433	MC1A	Oxhide	¼	18.902	15.690	38.918	0.83	72.8	6.16	12.5	209.9	373.4	23.9	0.09	5.63	0.79	29.3	20.6	0.00	0.04	17.97	1.35	2918.4	53.5	0.01
KW 3703	MC1A	Slab	Fragment	18.917	15.709	38.985	0.61	43.3	6.24	11.0	209.4	450.1	25.8	0.08	5.58	0.27	30.4	24.7	0.87	0.05	11.14	1.34	2971.9	55.6	0.01
KW 3934	P1	Fragment	Fragment	20.046	15.736	38.727	0.51	20.5	6.22	13.3	69.1	186.1	15.3	0.02	0.47	0.46	34.4	12.6	0.77	0.01	4.16	0.37	24.2	24.9	0.02
KW 3935	MC1A	Anchor	Full	18.948	15.704	38.988	0.79	20.8	6.65	14.2	650.1	261.6	25.4	0.34	7.87	0.70	29.6	21.4	1.61	0.43	23.05	0.36	1780.0	56.8	0.01
KW 4000	MC1A	Slab	Full	18.951	15.746	39.120	1.05	41.8	6.28	17.9	1196.5	358.6	20.8	0.02	2.58	0.84	23.9	23.3	0.00	0.01	1.94	0.26	951.6	36.4	0.01
KW 4166	P1	Oxhide	¼	19.196	15.649	38.349	0.72	34.1	7.42	25.9	122.0	444.5	17.1	0.03	0.57	0.79	36.5	16.4	4.53	0.04	0.76	7.67	44.3	57.8	0.02
KW 4265	P1	Oxhide	¼	19.080	15.685	38.588	0.76	11.9	6.19	11.0	84.4	165.8	27.7	0.02	0.46	0.35	30.6	10.9	1.05	0.01	0.86	2.08	44.7	49.8	0.06
KW 4267	MC1C	Slab	Full	18.950	15.661	38.814	-0.27	184.0	6.91	60.6	663.8	243.5	9.6	0.03	0.89	0.62	27.8	14.6	1.07	0.01	1.43	1.05	183.5	46.0	0.01
KW 4388	P1	Oxhide	¼	19.574	15.690	38.465	0.89	25.5	7.39	22.7	135.9	383.8	23.5	0.02	0.64	0.84	41.5	14.2	5.82	0.01	1.65	0.79	89.4	57.8	0.01
KW 4419	MC1A	Oxhide	¼	19.014	15.699	38.990	0.51	35.5	6.88	15.9	130.8	335.8	20.2	0.01	0.78	0.58	36.1	11.1	0.61	0.01	0.83	0.65	444.2	49.0	0.01
KW 4469	MC1C	Oxhide	¼	18.976	15.685	38.972	-0.75	28.2	6.54	23.1	80.1	233.1	15.1	0.01	0.49	0.34	30.9	21.2	9.57	0.01	0.61	0.41	305.0	33.8	0.01
KW 4484	MC1B	Oxhide	¼	20.000	15.868	38.965	0.52	15.9	6.33	23.8	91.9	157.0	22.3	0.06	0.47	0.40	31.7	11.2	0.00	0.01	0.80	0.31	260.7	43.5	0.02
KW 4485	MC1A	Oxhide	¼	19.015	15.697	38.986	1.22	50.8	6.18	10.1	108.5	286.1	20.5	0.01	2.09	0.56	25.2	11.2	0.12	0.01	5.14	0.27	1771.3	40.9	0.01
KW 4575	MC1A	Oxhide	¼	18.997	15.712	39.056	0.56	70.6	6.60	11.8	201.3	274.2	23.5	0.02	3.17	0.71	28.5	21.8	0.00	0.01	7.36	0.23	1848.3	48.1	0.01
KW 4576	MC1A	Oxhide	¼	18.988	15.706	39.024	0.79	70.6	6.60	27.1	201.3	274.2	23.5	0.02	3.17	0.71	28.5	26.0	2.83	0.01	7.36	0.23	1848.3	48.1	0.01
Lot 452	P1	Oxhide	¼	19.629	15.711	38.612	0.92	31.2	4.94	11.2	66.7	185.6	35.0	0.02	0.51	0.39	27.1	8.6	0.00	0.01	1.79	2.78	21.6	32.8	0.01
Lot 5552	P1	Fragment	Fragment	19.901	15.719	38.522	0.82	27.1	6.11	93.1	175.9	204.8	34.9	0.12	0.62	0.41	32.5	9.2	0.00	0.01	2.58	0.27	53.7	59.2	0.02
Lot 651	MC1A	Oxhide	¼	19.045	15.742	39.138	1.05	42.1	5.69	85.1	128.9	243.6	40.3	0.06	1.02	0.60	30.6	11.7	0.00	0.01	1.91	0.58	386.1	44.2	0.09
Lot 7331	MC1A	Oxhide	Ear	19.007	15.709	38.942	0.56	23.2	5.90	25.4	133.2	398.0	34.9	0.03	1.09	0.75	33.2	9.2	4.96	0.00	2.54	0.16	181.4	60.7	0.03
Lot 9263	MC1A	Slab	Corner	18.964	15.708	39.012	1.08	27.9	5.13	7.3	215.6	219.6	39.2	0.03	1.75	0.61	26.8	7.2	0.00	0.01	1.27	0.12	1075.4	50.8	0.07
Lot 9267	P1	Oxhide	¼	19.192	15.681	38.527	0.60	193.5	9.08	166.5	714.8	508.2	9.6	0.03	1.10	0.76	43.5	25.1	14.46	0.00	2.54	0.04	81.0	62.8	0.03

Figure S1: Cross-plots of Uluburun tin ingot compositions, A) Cu vs Au; B) Sb vs Te Analytical groupings correspond to isotopic and chemical composition correlated with age: MC=Mesozoic-Cenozoic, P=Paleozoic, Unk= Unknown; icon shape corresponds to ingot form; icon size reflects Pb concentration.